International Journal of Computer Integrated Manufacturing

ISSN: 0951-192X (Print) 1362-3052 (Online) Journal homepage: http://www.tandfonline.com/loi/tcim20

A novel path planning methodology for extrusion-based additive manufacturing of thin-walled parts

Yuan Jin, Yong He & Jianke Du

To cite this article: Yuan Jin, Yong He & Jianke Du (2017) A novel path planning methodology for extrusion-based additive manufacturing of thin-walled parts, International Journal of Computer Integrated Manufacturing, 30:12, 1301-1315, DOI: 10.1080/0951192X.2017.1307526

To link to this article: https://doi.org/10.1080/0951192X.2017.1307526

Published online: 22 Mar 2017.

International Journal of Computer Integrated Manufacturing, 2017
Vol. 30, No. 12, 1301–1315, https://doi.org/10.1080/0951192X.2017.1307526

A novel path planning methodology for extrusion-based additive manufacturing of thin-walled parts

Yuan Jin[a]*, Yong He[b] and Jianke Du[a]

[a]*School of Mechanical Engineering and Mechanics, Ningbo University, Ningbo, China;* [b]*School of Mechanical Engineering, Zhejiang University, Hangzhou, China*

(*Received 22 August 2016; accepted 12 March 2017*)

Extrusion-based layered deposition is one of the widely used additive manufacturing (AM) technologies due to its flexibility and capability in producing prototypes without geometrical complexity limitations. One of the most important steps in determining the part quality and build time is the path planning, where the trajectory for guiding the extruder is defined by various aspects prior to actual deposition. In this paper, a novel methodology is presented to generate the deposition path for the extrusion-based AM of thin-walled parts, which is difficult to obtain desirable deposition quality using general filling paths. A wavy path pattern is adopted to fill the long and narrow cross-sections that are obtained from the slicing procedure of the thin-walled parts. This novel filling pattern can bring in better deposition results and has more excellence in enhancing the efficiency. The algorithms are proposed for the generation of wavy paths at first. Then, several implementations and optimisation methods are proposed to address some issues and extend its application. Finally, two cases are used to verify the developed methodology, and the comparison analysis demonstrates its evident advantages over traditional filling path in the fabrication efficiency for the extrusion-based additive fabrication of thin-walled objects.

Keywords: extrusion-based additive manufacturing; path planning; wavy path; thin-walled parts

1. Introduction

Solid freeform fabrication, rapid prototyping and layered manufacturing were well-known names in the early stage for a family of production technologies that are currently grouped in the additive manufacturing (AM) (Valkenaers et al. 2013), or less formally as 3D printing, according to the definition given by ASTM International Committee F42 (Wohlers 2015). AM is an appropriate name to describe the technologies that integrates computer-aided design, computer numerical control, material science and process control to produce 3D objects by joining layer-upon-layer of material, whether the material is plastic, metal, powder, silicone, biocompatible hydrogel etc. The capabilities of AM technologies in lessening or avoiding some difficulties appearing in conventional manufacturing fabrication methods facilitate the diffusion of AM in a wide range of applications, such as prototype fabrication, product development, biomedical engineering, electronical devices, architecture etc. (Boschetto and Bottini 2016). Additionally, the advantages in reducing the development period and building parts without geometric constraints have attracted a surge of research interest in this area from various disciplines.

Extrusion-based AM, as presented in this work, is a subgroup of AM processes fabricating parts through the extrusion and deposition of material with a successive layer-by-layer process (Turner, Strong, and Gold 2014), where the material is first fed into a print head, or nozzle by the driving force from a step motor or pneumatics and then extruded from the nozzle tip. The extruded material is deposited on a platform to form a certain 2D shape according to the designed trajectory for the extruder and solidifies quickly to proceed the deposition of its upper layers. After one layer has been built successfully, the extruder would move relative to the platform in the build direction by a distance equal to the layer thickness to produce another layer, and finally to obtain 3D parts.

From the perspective of modelling and designing, AM of an object starts from a digital model, commonly represented by tessellated format that can be obtained from a CAD model or the scanned point cloud (Kai, Jacob, and Mei 1997a, 1997b). The virtual model is subsequently processed with several certain steps into a large number of slices; the number of the slices is dependent on the layer thickness, which has a significant influence on the fabrication resolution and the build time. To conquer the conflict between these two aspects, adaptive slicing schemes were proposed by adaptively changing the layer thickness in the slicing procedure depending on the geometric characteristic of the 3D model (Huang and Singamneni 2013; Wang et al. 2015). After that, a filling path pattern is applied to each layer to cover all the areas to be filled and the designed paths are exported as codes that can be recognised by the machines. In the path

*Corresponding author. Email: jinyuan@nbu.edu.cn

planning process, several factors are required to be considered, such as deposition quality, fabrication efficiency, number of sub-paths, linking sequence and so on (Cerit and Lazoglu 2011; Chou, Chen, and Chou 2008; Weidong 2009). Besides, in the designing process of extrusion-based AM, support structure is necessary for assisting in building parts with overhang features and would be removed afterwards (Huang et al. 2009).

In the aforementioned process steps, path planning is one of crucial tasks for the extrusion-based AM by determining the trajectory for the deposition head to fill the cross-sectional shape of one specific 2D layer (Ding et al. 2015). The generation of paths is comprised two main steps: filling the interior areas and linking the sub-paths. The interior filling refers to how to fill up the internal area defined by several boundaries continuously without stopping and restarting the extrusion and deposition process, while the linking method is more about determining the connecting sequence of the sub-paths. Although many efforts have been exerted to these two aspects, there are still many shortcomings and limitations in handling with increasingly complicated geometries in terms of filling quality and deposition efficiency. In the generation of interior filling paths, overfill and underfill phenomenon usually appear near sharp corners and different geometries of the cross-sectional shape require different filling patterns. When determining the linking sequence of the generated infilling sub-paths, the less number of sub-paths would result in better deposition effect.

Kao and Prinz (1998) pointed out that there was no room for improving the deposition quality by producing a completely smooth, connected spiral path that fills entirely a given arbitrary cross-sectional geometry without overlapping, then a shape optimisation algorithm was proposed to be implemented in a way that high-quality spiral deposition paths could be produced based on its skeleton. Han et al. (2002) proposed a grouping and mapping algorithm-based deposition planning approach according to the underfill and overfill analysis. The main idea of the approach was to group the adjacent vector segments according to their similarities and assign an appropriate flowrate to each group using linearised mapping functions and the road geometry could be kept constant by adjusting the roller speed during the deposition process theoretically. Yang et al. (2002) presented an equidistant path generation algorithm to bring significant improvements to the AM process both in processing efficiency and part quality. In the connection between sub-paths, Wah et al. (2002) employed a combination of Asymmetric Traveling Salesman Problem and Integer Programming to solve this problem to minimise the time wasted on non-deposition motions. While Tang and Pang (2003) pointed out that significant time might be wasted in the movement between the end point of one sub-path to the start point of the next one and a maximum linear intersection algorithm as well as a variation of the Generic Algorithm was proposed to solve this problem. Jin et al. (2014b) proposed some strategies to decrease the number of useless path elements for the zigzag paths. They also (Jin et al., 2014a) developed a method for the fused deposition modelling to improve the depositing quality by confirming equidistance between the path elements within the subregion by means of adjusting their locations adaptively and locally.

So far, the most popular fill methods used in current AM systems are based on either direction parallel or contour parallel-based patterns (Zhao et al. 2016). The direction-parallel path is consisted of a series of parallel segments along a specified direction, which should be selected to minimise toolpath length and maximise average toolpath element length (El-Midany, Elkeran, and Tawfik 2006). After the direction of the sweeping lines has been determined, connected paths are generated by linking all the segments that are obtained from the intersections between sweeping lines and the boundary of input geometry. So, the obtained direction-parallel path contains many segments correspond to back and forth motion along a fixed direction within the boundary to fill up the interior area. Many related algorithms and approaches on the generation of direction parallel-based path have be developed in conventional CNC pocket milling and can be used in the extrusion-based AM with a few modifications (Held 1991; Kim 2010; Park and Choi 2000). In contrast, contour-parallel paths are comprised a set of closed contours parallel to the boundaries of a given 2D geometry (El-Midany, Elkeran, and Tawfik 2006). The key in the generation of contour parallel-based paths is the implementation of the offset algorithm, which is commonly computationally expensive. The offset process of a contour can be defined as the offset of a set of sampling points with a constant distance along their normal from the original contour. Actually, the offset algorithms have been widely studied as a typical CAD/CAM problem and many algorithms are now available for the offsetting process (Lin et al. 2013; Liu et al. 2007; You, Sheen, and Lin 2001). After the offset contours have been obtained, several patterns can be generated, such as spiral (Lee 2003), double spiral (Zhou et al. 2016) and connected Fermat Spirals (Zhao et al. 2016). The fill paths based on the above two standard patterns tend to bring the discontinuity and non-uniform deposition issues when handling with complex 2D cross-sections with many long and narrow areas. This can be demonstrated in Figure 1, the direction parallel-based path used in this type of shape would result in many sharp corners and thus jeopardise the deposition quality, while many overfill or underfill issues would appear when the width of the area changes continuously with the contour parallel-based path. The final paths are comprised several sub-paths under both circumstances.

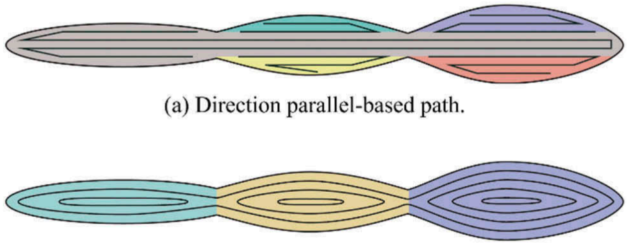

(a) Direction parallel-based path.

(b) Contour parallel-based path.

Figure 1. Two standard fill path patterns. (a) Direction parallel-based path; (b) contour parallel-based path.

Besides above two basic patterns, several strategies and methods have been developed for the path generation of AM. Jin et al. (2013) developed a hybrid and adaptive path generation approach to improve geometrical accuracy and build time by using the contour parallel-based paths to fabricate the boundary and neighbouring regions of each sliced layer to preserve geometrical accuracy, while adopting the zigzag paths for the internal region of the layer to simplify computing processes and speed up fabrication. Ding et al. (2014) presented an algorithm to generate optimal paths for the wire and arc AM with three steps. The first step was to decompose the 2D geometries into a set of convex polygons based on a divide-and-conquer strategy; then, an optimal scan direction was identified and a continuous tool-path was generated using a combination of zigzag and contour pattern strategies for each polygon; finally, all individual sub-paths were connected to form a continuous curve. This strategy could result in better surface accuracy compared with the existing hybrid method. Zhao et al. (2016) developed a new kind of fill path pattern, which use the connected Fermat spirals to fill the whole region with one single connected path. The generated paths had the property of long, low-curvature and continuity, which had positive effects on the quality and efficiency of AM. Steuben, Iliopoulos, and Michopoulos (2016) proposed a novel implicit algorithm based on the computation of paths derived from the level sets of arbitrary heuristics-based or physics-based fields defined over the input geometry. The method computed the paths based on the solution to differential equations defined on the implicit layer regions; so, it allowed for a straightforward implementation that avoids the complexity associated with traditional polygon offsetting and offered great flexibility in the specification of the path for AM. With the increasingly high demand for algorithm implementation and part performance, more novel and optimised path generation methods are being under development.

Thin-walled structures are very common in complex models and still cannot achieve desirable deposition results using conventional fill paths in AM. More novel path generation method is required to further improve the fabrication quality and enhance the efficiency. There have been some related researches in the fabrication of thin-walled part with AM technologies. Peng et al. (2007) introduced an open-loop direct laser fabrication process to fabricate thin-walled parts of nickel alloy and the process parameters and special control method for improving the shape quality of single-bead walls and complex thin-walled parts were investigated in detail. Abele et al. (2015) studied the generation of thin-walled elements with defined porosity characteristics using selective laser melting and tried to improve the porosity, pore size distribution and permeability of thin-walled parts by the optimisation of a variety of process parameters. Alexander and Dutta (2000) proposed a local wall thickening method to manufacture sheet surfaces by considering the accuracy of only one side. This strategy could preserve the accuracy of the accurate side while reducing the total material and build time during manufacture by avoiding the use of supports. Ding et al. (2015) presented a gap-free path planning methodology for AM process by offsetting the medial axis of the given geometry towards its boundary. And, this gap-free path could significantly improve the quality of the fabricated components partially for thin-walled structures.

In this paper, a novel methodology to generate deposition paths for thin-walled parts is presented. First, a wavy path pattern is introduced for filling long and narrow shapes to address the deposition issues appearing in general direction parallel and contour parallel-based paths. Second, six steps are involved to generate the medial axis-based wavy path for long and narrow cross-sections. Then, several optimisation methods are proposed to improve the deposition performance and to extend the application of wavy path in building 3D thin-walled models. At last, two examples are used to verify the developed methodologies, and the results show that the proposed approaches and strategies are effective for the extrusion-based additive fabrication of thin-walled objects. The remainder of this paper is organised as follows: Section 2 introduces the wavy path pattern and describes the generation algorithms in detail. Section 3 presents the implementation and some optimisations. Two case studies are conducted in Section 4, followed by some conclusions in the last section.

2. A novel path planning methodology

In this section, a novel path pattern is introduced to fill the cross-sections sliced from the thin-walled parts. The geometry of this type of cross-sections commonly has long and narrow shape and thus cannot achieve desirable deposition results using general fill path patterns in the extrusion-based AM. The main reason is that the width of the shape to be filled is so small that the evenness and uniformity is very difficult to achieve within one layer and between layers.

2.1. Wavy path pattern

In order to address the aforementioned issues in depositing long and narrow geometries, wavy path pattern is developed in our work. As illustrated in Figure 2, the initial demonstration involved several simple thin-walled objects where every layer from the slicing procedure is deposited with the wavy path pattern. It can be seen that each 2D slice of the thin-walled part can be built with two types of path element: the path along the offset contour of initial input geometry and the wavy path inside the contour. The path along the contour of the sliced cross-section is used to preserve the shape and achieve the geometrical accuracy, while the wavy path can fill the internal area relatively uniform and pretty fast. There should be some overlaps between these two path elements to enhance the bonding strength, and thus to achieve desirable mechanical performance of the deposited thin-walled part. On the other hand, the deposited paths between adjacent layers are supposed to be joined well to build the whole 3D thin-walled part successfully.

It is obvious that the novel wavy path pattern can bring in significant reduction in the material use and build time to fill this type of cross-section since much shorter paths are required compared to other conventional path patterns. Additionally, the biggest advantage of this path is the number of sub-paths which can be decreased to minimum that is beneficial for the extrusion-based AM from several perspectives. Specifically, the task for the interior filling of a closed long and narrow shape can be accomplished with only one wavy path regardless of the complexity of the geometry. Besides, the wavy path sometimes can be connected to the contour path to further decrease the number of sub-paths. The mechanical performance of the part stacked with many layers of wavy path is largely affected by some geometric parameters, such as the amplitude and the period length, which are crucial to define the shape of the wavy path.

In the wavy path, the amplitude can be defined as the distance between the wave peaks (or troughs) and a centre line that goes through the whole wave, while the period length is the distance between two intersections of the wavy path and the centre line. These two parameters can affect the weight and strength distribution of the fabricated parts markedly; so, determining them is important for the generation of the wavy path based on the input geometry. This work will be discussed in the next section. Besides these two geometric parameters, the distribution of the wave peaks (or troughs) is also very critical. The contour connecting all the peaks (or troughs) is defined as the peak contour (trough contour). So, the distribution of the wavy peaks can be quantified as the length between adjacent peaks along the peak contour. The same quantitative method is adopted to describe the trough distribution. At the same time, in case the strength at two ends of the

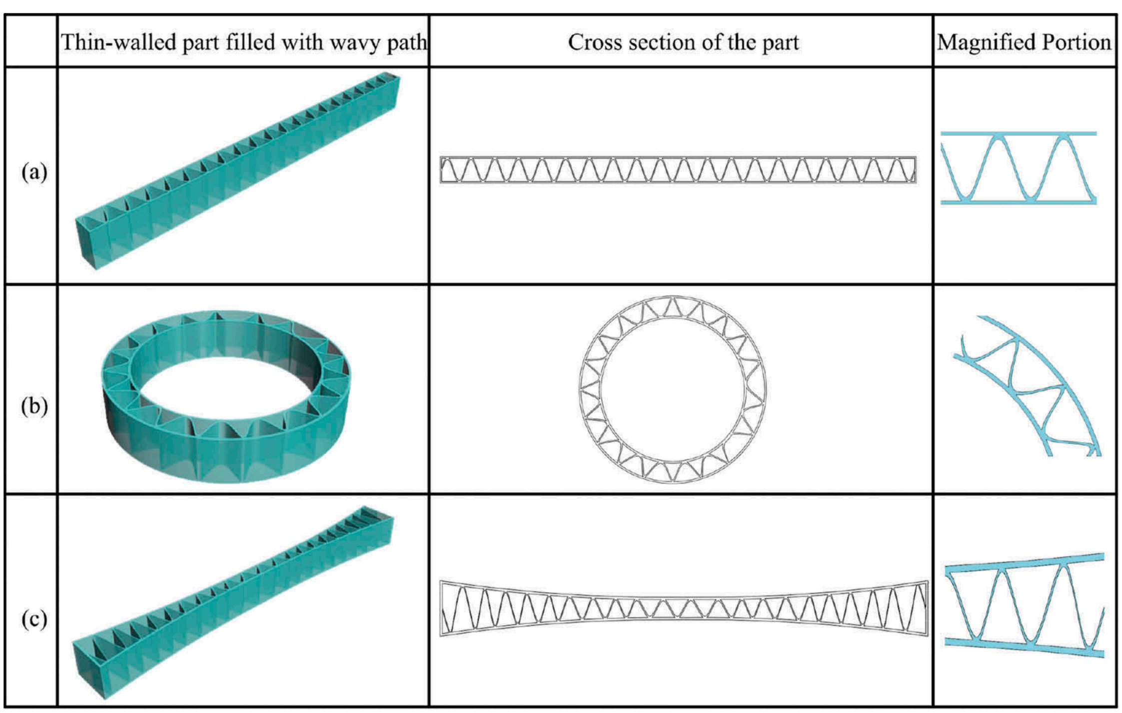

Figure 2. Demonstration of wavy path pattern for filling thin-walled parts.

shape is too weak to bear the load perpendicular to the ends, the starting and ending points of the wavy path are selected at the midpoint of the side, just as shown in Figure 2(a) and (c).

The thin-walled part in Figure 2(a) is a basic and simple shape where the amplitude and the period length of the wavy path keep constant and the same case in the ring-like part of Figure 2(b). However, despite the peak distribution and the rough distribution are the same in the shape of Figure 2(a) since the shape is symmetrical to the centre line of the wavy path, it is not the case in the shape of Figure 2(b), where the peaks and the troughs are distributed evenly along the peak contour and the trough contour, respectively. As for the thin-walled part in Figure 2(c), the amplitude of the wavy path changes according to the geometry of the boundary, and the period length and the distribution of the peaks and troughs are modulated locally by considering the influence on the weight distribution and part strength.

According to the demonstration of wavy paths used in these three thin-walled parts, the generation of the wavy path for one layer can be roughly accomplished by the following steps: get the centre line of the shape, determine the period length on the centre line, generate the peak points and trough points on the peak contour and trough contour based on the points on the centre line, link all the peak points and trough points sequentially to generate the wavy path. Therefore, the first step is to obtain the centre line of the cross-section, which is termed as medial axis geometrically and computationally.

2.2. *Medial axis transform*

Medial axis transform (MAT) of a 2D shape can be used to concisely represent the domain shape and is very useful for analysing the complex domain. The MAT is based on the medial axis, which geometrically bisects the domain and becomes the shape skeleton (Chen and Fu 2011). So, the medial axis is also known as the skeleton. As shown in Figure 3, the medial axis is bounded by the planar curve

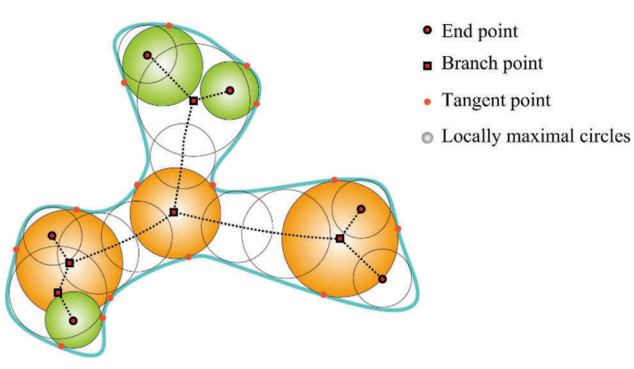

Figure 3. Illustration of the medial axis of a 2D shape.

and is the set of the locus of centres of locally maximal circles that are tangent to the curve in two or more points. The dot lines are the medial axis of the input geometry. The medial axis of a simple polygon can be visually described as a tree whose leaves are the vertices of the polygon, while the edges are either straight segments or arcs of parabolas (Blum 1967).

Together with the associated radius function of the maximally inscribed circles, the medial axis is called as the MAT, which is a complete shape descriptor and can be used to reconstruct the shape of the original domain (Lee 1982). So, the geometric information of MAT allows the generation of wavy path inside the domain. The computation of MAT has very higher computational complexity and thus has been widely studied over the past few decades. Currently, however, the majority of algorithms for computing the medial axis of a simple, nondegenerate polygon are still relatively computational expensive. Fortunately, a straightforward implementation of the MAT for 2D polygons is provided by the CGAL C++ library (Cacciola 2004); our related algorithms are implemented based on this open library.

2.3. *Wavy path planning*

As illustrated in Figure 4, it is shown how to generate the wavy path based on the input geometry sliced from a thin-walled part. The flowchart of the algorithms consists of three major steps: In the first step, the CAD file of the thin-walled model is read and two basic operations are applied on the model: orientation determination and slicing. The sliced layers are exported for the subsequent steps. The second step is the generation of the wavy path, including six sub-steps. Postprocessing is applied to the generated wavy path in the third step to allow for the manufacture of the whole 3D thin-walled object. The algorithms of step 2 are detailed in this section, while the details of step 1 and step 3 are not presented here since they are the same with other path generation methods and have been well studied.

The thin-walled part in Figure 5(a) is used to illustrate the wavy path generation process. The imported digital model undergoes a preprocessing, where its build and slicing orientation are determined for the subsequent slicing first. In the slicing procedure, a set of parallel planes is adopted to intersect with the model and a group of cross-sections of the model is obtained as shown in Figure 5(b) and (c). All the cross-sectional geometries are sent to the next module to generate the wavy path layer by layer.

For the 2D geometry of one sliced layer, an offsetting operation is applied to obtain the contour for the generation of the wavy path as shown in Figure 6(a). The offset distance is the given path gap w which is determined based on some parameters, such as the diameter of the

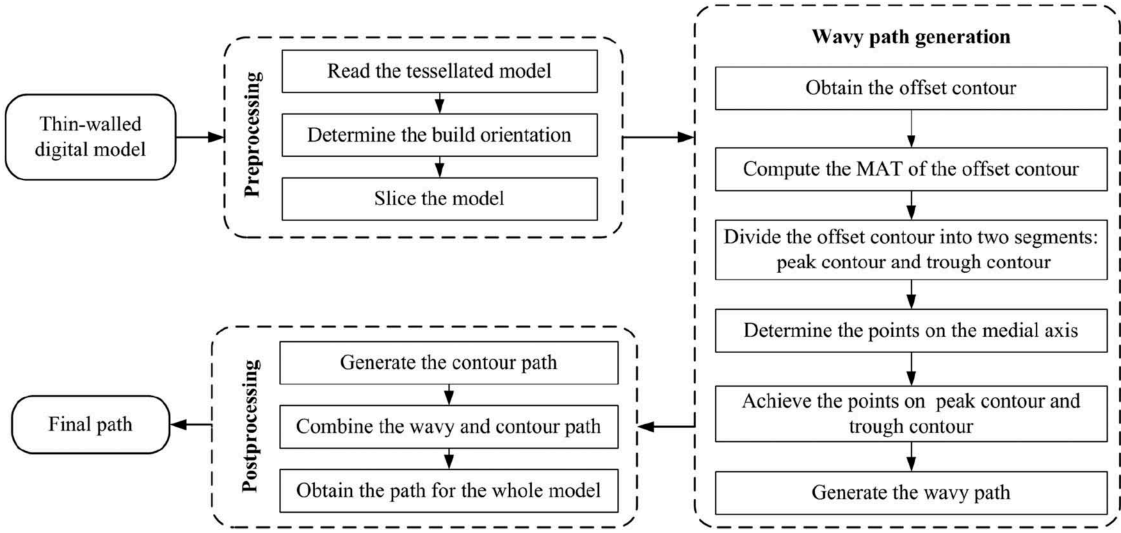

Figure 4. Flowchart of the developed path planning method for thin-walled parts.

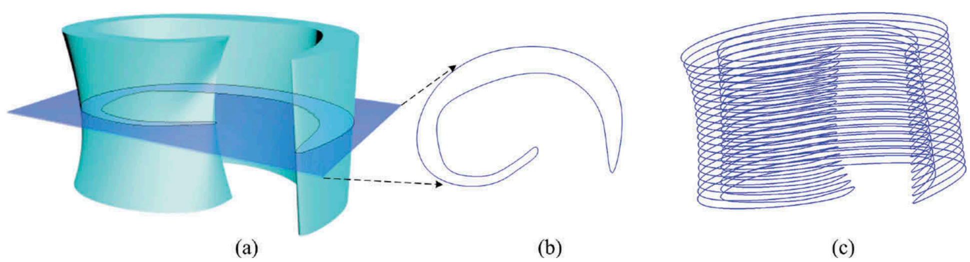

Figure 5. The preprocssing step of a thin-walled part model.

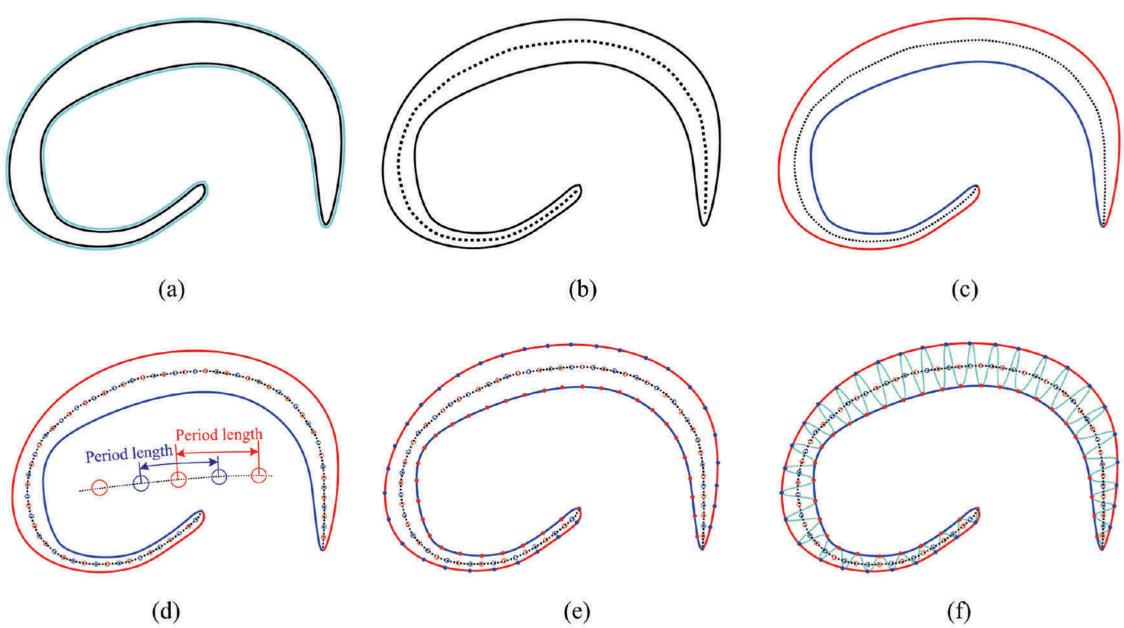

Figure 6. Illustration of the wavy path generation process.

nozzle tip and the associated layer thickness. The number of offsetting loops would directly affect the accuracy and the mechanical strength of the outer boundary and is commonly dependent on the user preference. In this study, only one offsetting is adopted for illustrative purpose.

After obtaining the offset contour, the MAT of this contour is computed. It can be observed from Figure 3 that there are two types of the point in the generated medial axis: branch point and end point. The main task of this step is to find a no-branched skeleton of the offset contour, meaning that the final skeleton cannot contain any branches. In other words, there must be two and only two branches for any branch point at the final skeleton. So, redundant branches at the branch points of the medial axis from MAT are supposed to be removed. Once a branch is selected to be eliminated, all the end points and branch points inherited from this branch are all removed. The selection of the branches to be removed is based on the following rule: if the length of one branch is smaller than another branch, this branch is removed. Here, the maximal length between the branch point and its children end points is defined as the length of this branch. This can be illustrated in Figure 7, the left is the contour skeleton from the MAT and there are four branch points in the medial axis that have more two branches. At branch point **A**, there are three branches, and it is obvious that the length between $\mathbf{A_2}$ and **A** is smaller than that between $\mathbf{A_1}$ and **A**, so the branch $\mathbf{A}$–$\mathbf{A_2}$ is removed. There are totally four branches at point **B**, so there should be two branches to be pruned. With comparative analysis, the branches $\mathbf{B}$–$\mathbf{B_1}$ and $\mathbf{B}$–$\mathbf{B_2}$ are removed together. It should be noted that all the points inherited from $\mathbf{B_1}$ are removed (such as $\mathbf{B_{11}}$ and $\mathbf{C_{11}}$ in the example). The same operations are applied on branch point **C** and **D**, and the final no-branched skeleton is as shown in the right of Figure 7.

With the obtained no-branched skeleton, the contour is going to be divided into two segments. There are two possible situations when handling the input geometry. The first situation is the input geometry which is a simply connected region, which has no holes inside the boundary, while the second situation is that the input long and narrow shape is comprised two contours: internal contour and external contour. Under the latter situation, the generated skeleton must be a closed loop and there is no need for contour division. But in the former situation, the input contour is a closed loop and can be separated by the two ends of the skeleton into two segments. So, the task of this step is transferred to find out two points on the contour based on the relation between the skeleton and the contour.

There are three possible cases to get the separating point as illustrated in Figure 8. The first case in Figure 8(a) is that one of the end points of the skeleton is on the contour; then, this point is namely one of separating points. If the end point is not on the contour as shown in

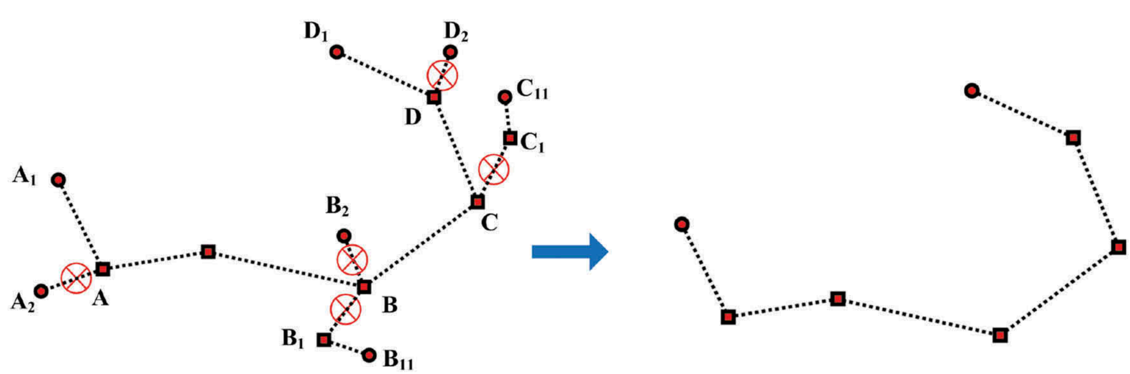

Figure 7. Removal process of the redundant branches.

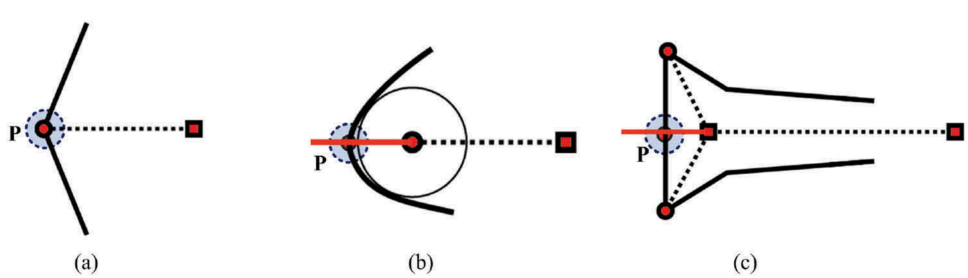

Figure 8. Calculation process of separating point under different cases.

Figure 8(b), an extended line is drawn to intersect with the contour and the intersection is the separating point **P**. The generation of the separating points for the contours in Figure 6(c) belongs to this case. The last case appears when the last branch point on the skeleton has two end points that have the same or almost the same branch length. Under this case, the intersection between the contour and the bisector of the angle constructed with two end points and the branch point is the separating point as shown in Figure 8(c). One of the separated segments of the contour is called as peak contour and the other is called as trough contour for easy to distinguish.

The next step is to generate the sampling points evenly on the skeleton based on a proper period length λ, which is dependent on the material property and the strength requirement. The period length can be easily modified and have no effect on the generation process of wavy path; so, this part is not detailed in our study and the results are shown in Figure 6(d). Based on the sampling points on the skeleton, the corresponding points on the peak contour and trough contour could be initially generated directly from the definition of the medial axis. Specifically, maximal inscribed circles can be drawn with the sample points as the centre; the tangent points on the contour are the corresponding points. This process can be seen from Figure 9. The obtained peak points and trough points are further spaced more evenly apart on the peak contour and the trough contour.

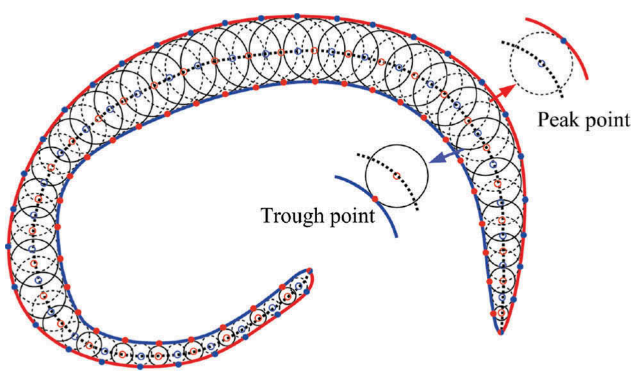

Figure 9. Generation process of peak points and rough points.

The last step is to connect all the points on the peak contour and the trough contour alternately using a spline curve. It should be noted that the two separating points are the start and the end points of the spline, respectively. The generated wavy spline is shown in Figure 6(f).

Using the aforementioned six steps to generate the wavy path for the long and narrow geometry of all the layers, the paths for the whole thin-walled part would be generated by combining all the sliced layers as shown in Figure 10. However, the shape in the illustration is very simple and there are some limitations and further works need to be addressed. For example, the computation of MAT is so time expensive that the whole process for all the sliced layers would be very time consuming; the large deviation between the wavy paths on adjacent layers would bring in the collapse of upper layer during the depositing process; how to improve the mechanical strength besides the method of adjusting the period length; the wavy path generation method should be extended to enable it to be applicable to the fabrication of arbitrary thin-walled parts. These limitations will be discussed and solved in the next section.

3. Implementation and optimisations

3.1. Uniformity between layers

In order to achieve the uniformity of the wavy path between layers, global optimisation can be performed using the geometry of all slices to adjust the location of peak points and trough points. But the computation for the global optimisation would be very time consuming since the number of sliced layers is quite large. In this study, a local optimisation method reported by Reiner et al. (2014) is adopted to reduce the consumption of memory and time. This method just requires the geometric information of the previous layer when determining the peak points and trough points of the current layer. A projection and relaxation process is iteratively performed on each layer from bottom to top.

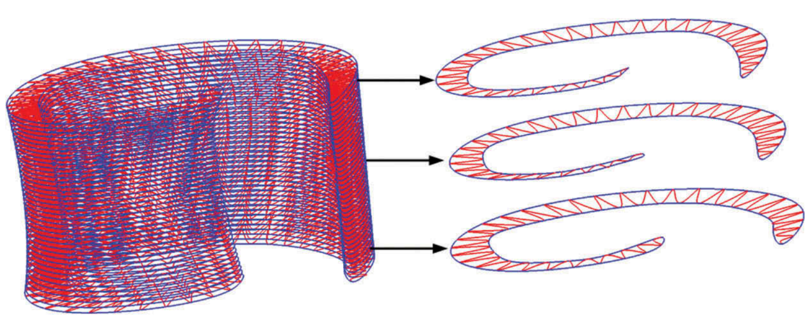

Figure 10. The final deposition paths combining the wavy paths of all the sliced layers.

Initially, an assignment of peak points and trough points is performed for the base layer based on the methods described in the last section; then, the projection and relaxation process is applied on all subsequent layers until the top of the thin-walled model is reached. Next, with the given peak points and trough points on the base layer, they are projected onto the associated contour of its upper layer, except those points whose distance is large that a certain value with its projected point. Specifically, the peak points are projected to the peak contour, while the trough points are projected to the trough contour. After all the projected points on the next layer have been obtained, their locations are relaxed and spaced evenly apart along the contour while the horizontal deviation between the point and its corresponding point on the former layer should be smaller than a certain threshold to avoid excessive malposition between them. Then, the point that has a distance much less than the period length with its adjacent points would be removed, while extra points would be inserted evenly on the empty segment between two points whose relative distance is longer than two times of the period length to enable the length between adjacent points is nearly equal to the period length. All the peak and trough points, including the newly inserted points while not including the deleted points, are relocated to achieve a better space.

By performing the above process for all the remaining layers, the peak points and the trough points are along a series of trace lines vertically as shown in Figure 11. The horizontal distance between associated points on adjacent layers would be restricted to a threshold; so, the uniformity between layers can be perfectly achieved with this method. At the same time, this method to determine the peak points and trough points could avoid the computation of MAT for every layer; so, the whole process would have higher efficiency.

3.2. *Dual-wavy path*

The above-generated wavy path for a simple connect area only consists of one wave, which is termed as single-wavy path in our study. As contrast, dual-wavy path is developed to provide more flexibility in the path generation and the final deposition performance. The generation of dual-wavy path just requires some modifications based on the single-wavy path generation process. Specifically, in the determination of the sampling points on the peak contour and the trough contours, each maximal inscribed circle has two tangent points on the contour. In the generation of single-wavy path, only one tangent point is adopted for the subsequent generation of wavy path as shown in Figure 9. However, the information of two tangent points are both utilised in the generation of dual-wavy path. Except those points that have been used to generate the single-wave path, the remaining points can be also used to generate another wave. The start point and the end point of two wavy paths are at the same locations (the separating points on the contour actually) if the original contour is separated by the separating points. Figure 12 shows two examples of the dual-wavy path. The mechanical strength of dual-wavy path is markedly better than that using single-wavy path.

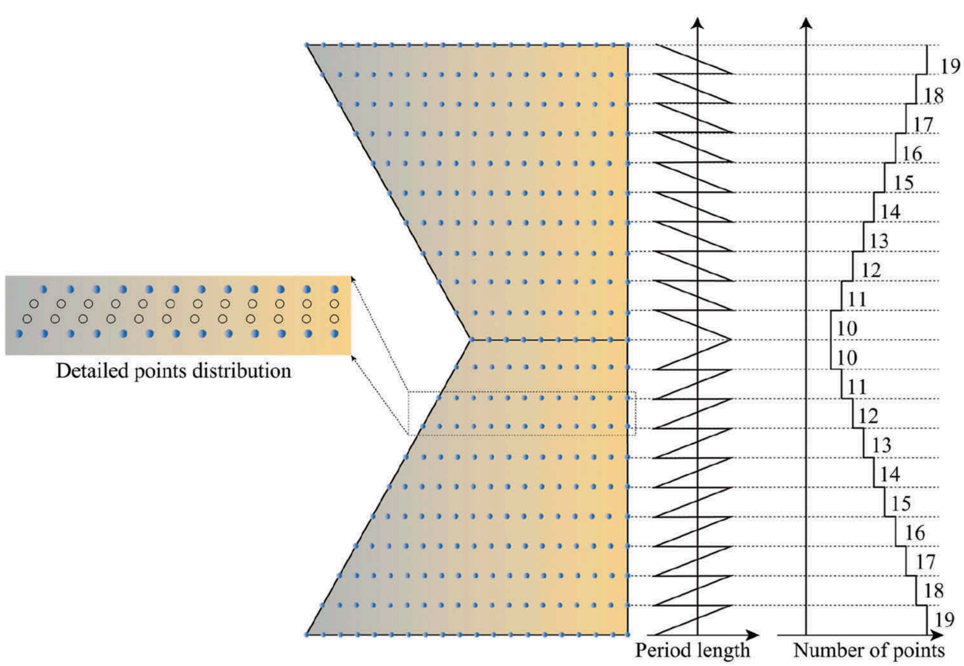

Figure 11. The obtained trace lines for the peak points of each layer.

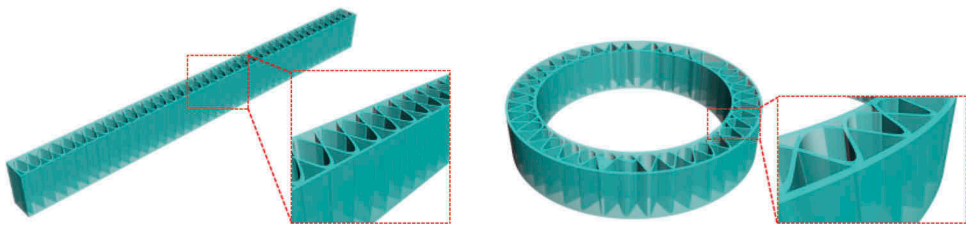

Figure 12. Demonstration of dual-wavy path.

3.3. Branched wavy paths

So far, the proposed wavy path generation method is only applicable to simply connected regions that have only one no-branched skeleton; this would definitely restrict the universal application of this novel path pattern. In this paper, some studies are conducted to facilitate the application of the proposed path generation methodology to more general thin-walled parts.

In processing the cross-sections of branched thin-walled parts, the majority of steps are the same with that in the generation of wavy path for no-branched geometries, but there are two major differences between them. The first difference is the generation of the skeleton of the contour; a threshold of the branch length is set to remove the redundant branches instead of removing all the shorter branches to obtain a no-branched skeleton in the simply connected region. The branches whose length is smaller than the given threshold are amputated, while the branches whose lengths are longer would be left for the subsequent wavy path generation. The obtained skeleton is then divided into several no-branched segments, which can be processed using the methodologies described in Section 3. As for the second difference, an additional step is required to connect all the sub-wavy paths. In order to enhance the connecting performance, the connecting point is supposed to locate at the peak or trough point of one wavy path, which can be achieved by adjusting the start or end point of one sub-wavy path adaptively. A simple demonstration of the wavy paths for branched thin-walled parts is shown in Figure 13.

With the wavy path generation methods for both no-branched regions and branched geometries having been proposed, arbitrary thin-walled models can be processed by decomposing the 2D cross-section of sliced layers into several regions, which can be filled by either no-branched wavy path or branched wavy paths. This will be demonstrated with an example in Section 4.

4. Result and discussion

The wavy path generation methodology described in the previous sections was implemented on two example thin-walled parts in Figures 14 and 18 using C++ language. A laptop computer with 4 GB memory was used to execute the developed program. The layer thickness is set to be 0.3 mm for the slicing procedure and the path gap for the offsetting process is 0.5 mm. For the estimation of the build time, the maximal deposition speed to fill the paths is 30 mm/s and the acceleration is 100 mm/s^2 to calculate the time in the accelerating and decelerating processes.

The first thin-walled model, whose cross-section can be represented with only one skeleton, is shown in Figure 14(a). The height of the model is 60 mm; so, the layer number is 200. The goal of this test is to apply the wavy path to simply connected regions and the show how to determine the peak points and trough points for the base layer and its upper layers. In order to preserve the exterior shape of the fabricated part, the bottom layers and top layers should be filled with dense pattern, such as zigzag or contour paths. Except those bottom layers and top layers, the intermediate layers are filled with wavy paths. In the generation of the wavy path

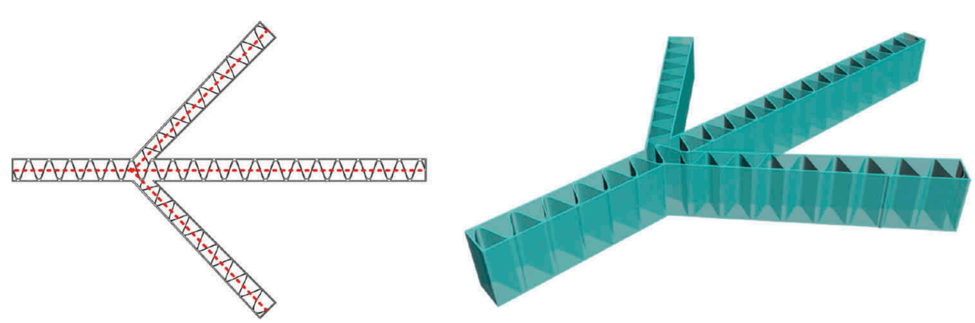

Figure 13. Demonstration of wavy path for branched thin-walled part.

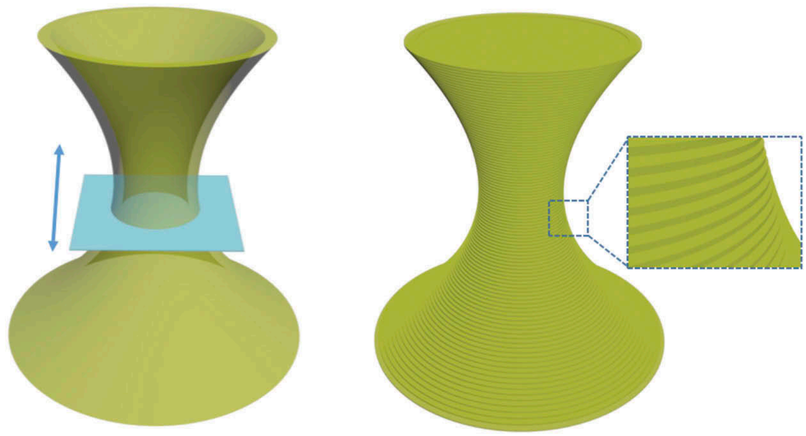

Figure 14. The example thin-walled part and its sliced layers.

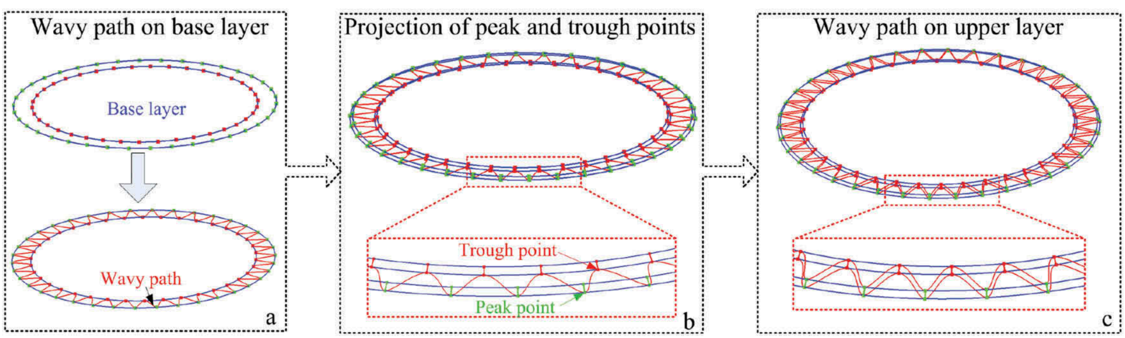

Figure 15. Demonstration of wavy path generation.

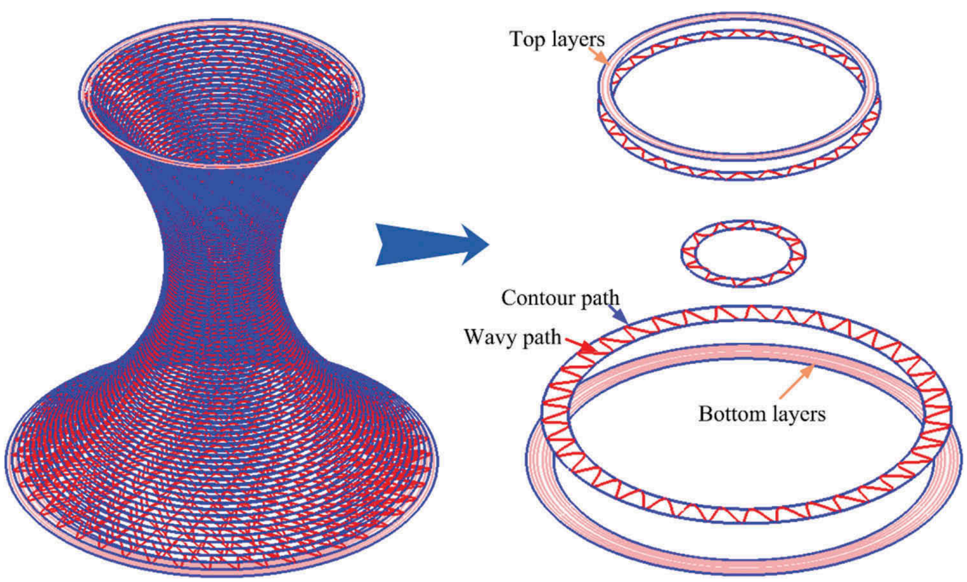

Figure 16. The output path for (a) the whole part and (b) sliced layers at different locations.

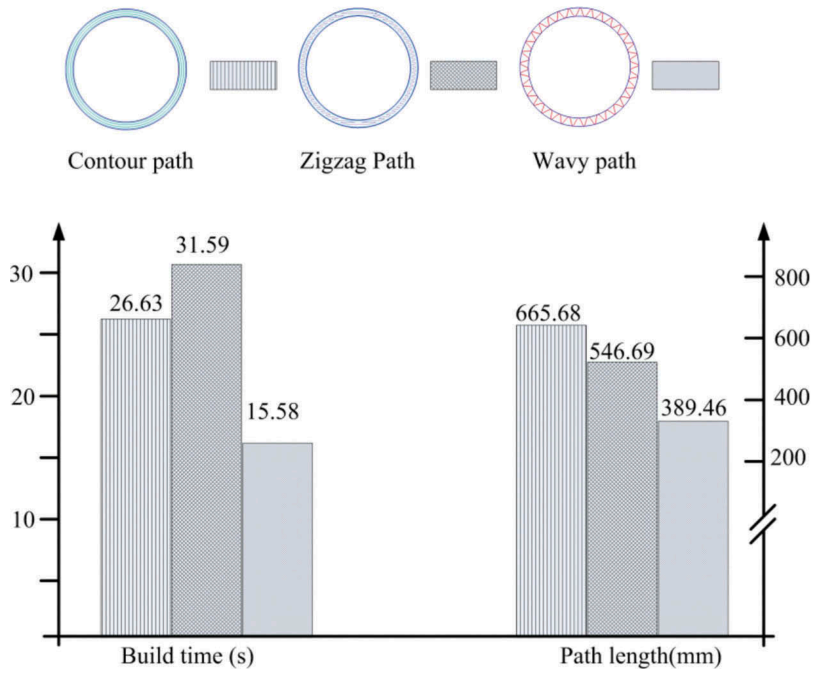

Figure 17. Comparison of build time and path length between different path patterns in example 1.

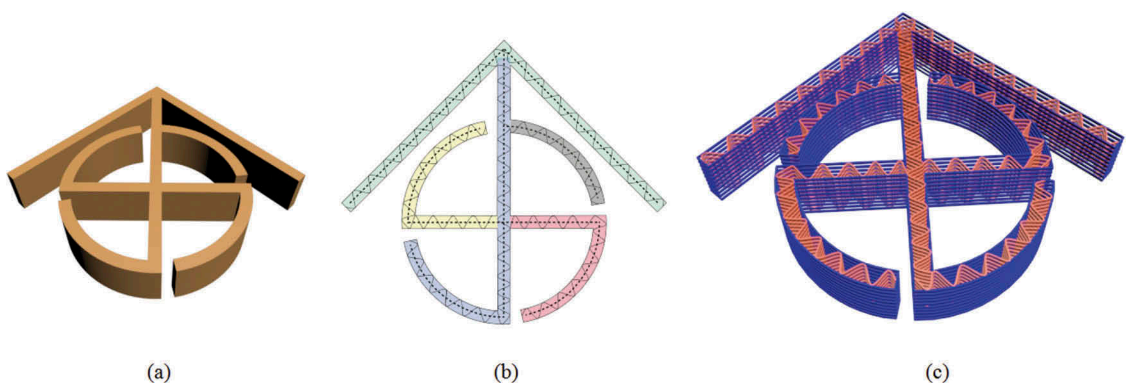

Figure 18. Demonstration of wavy path generation for a branched thin-walled part.

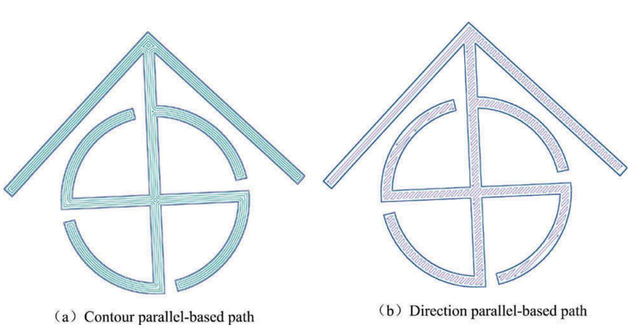

Figure 19. Demonstration of two general path patterns. (a) Contour parallel-based path; (b) direction parallel-based path.

for the base layer, the medial axis of the offset contour can be easily obtained and subsequently used to determine the sampling points based on the period length, which is considered as 4 mm in this model. Then, the peak points and trough points would be obtained from the tangent points between the contour and maximal inscribed circles. At last, the generated wavy path based on the obtained peak points and trough points for the base layer is shown in Figure 15(a). The peak points and trough points on the base layer are then projected to its upper layer as shown in Figure 15(b) to generate the corresponding points for the generation of the spline-based wavy path for the next layer. After the wavy

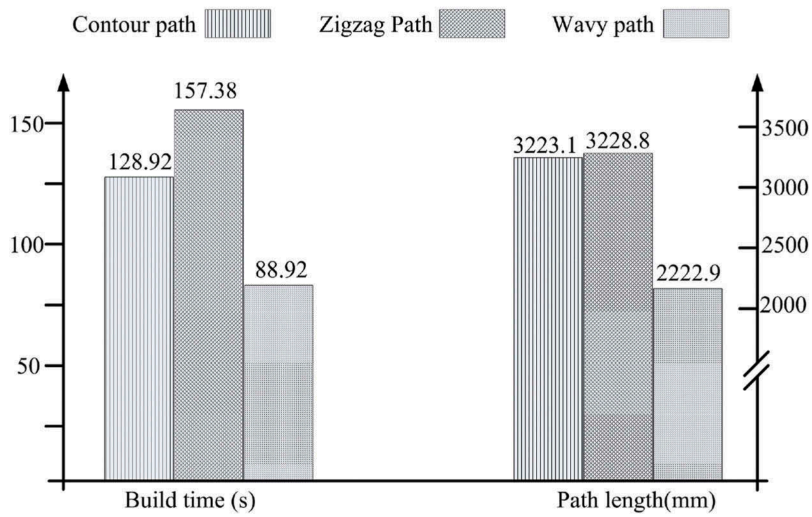

Figure 20. Comparison of build time and path length between different path patterns in example 2.

path for all the sliced layers having been achieved, all the path elements, including the outer contour paths and the wavy paths shown in Figure 16, are exported to generate the Gcode for the fabrication process.

The comparison of build time and material use for one layer between general path patterns and the proposed wavy path is shown in Figure 17. It can be seen that the adoption of the wavy path could bring in some reduction in the build time and material consumption. On the other hand, the filling path can be combined into only one path by properly choosing the start point; so, there is no useless path in the final paths. This is an evident advantage over other path patterns.

The second example object is a quite complex thin-walled part which is crisscrossed by a network of long and narrow shapes as shown in Figure 18(a). The purpose of this implementation is to demonstrate the application of the wavy path pattern to branched thin-walled objects, and to demonstrate the method of connecting sub-wavy paths. As the cross-sections of the whole thin-walled part have the same geometry, the generation of the wavy path is pretty straightforward by increasing the *z* coordination by a distance of the layer thickness after the path elements for the base layer have been obtained.

In the generation of the wavy path for the base layer, the medial axis of the offset contour is generated and some short and redundant segments are removed at first. Then, the skeleton is divided into several no-branched segments based on the branch points in the medial axis. Next, the initial wavy path for each segment is generated. At last, the connecting point between two wavy paths is supposed to at the peak point or trough point by locally adjusting the locations of associated peak points and trough points of one wavy path. The medial axis is divided into five segments and the connecting results between wavy paths are shown in Figure 18(b). The wavy path for the whole model is shown in Figure 18(c).

Likewise, the fabrication time and material use are compared with other two path patterns shown in Figure 19; the path gap for these two path patterns is 0.8 mm for the sparse filling. Figure 20 shows that the material is around 43% less than that with zigzag and 31% than contour parallel paths. And, the wavy path is over 31% quicker than other filling paths.

5. Conclusion

A novel methodology to generate deposition paths for thin-walled parts is developed in this paper. The geometric property of this new path pattern is introduced at fist to demonstrate its suitability in the deposition of the cross-section of thin-walled parts. Then, the detailed algorithms of the filling path generation are provided. Besides, in order to improve the deposition performance and to extend its potential application, several optimisation methods are further proposed. Finally, two case studies are conducted to verify the developed wavy path pattern and compare with other general path patterns, and the results show that the proposed approaches and methods are effective in the path generation for the fabrication of thin-walled parts. Therefore, the studies in this paper allow the additive manufacture of more complex models with thin-walled features faster and better.

Besides the material consumption and build time, the structural performance is another critical factor that should be considered in planning the deposition path. As the wavy path pattern brings in the continuous filament in the interior area rather than numerous corners, the flexural strength of fabricated parts is even better than that using common zigzag filling path pattern based on our recent research. In our ongoing research, the influence on the part strength from relative parameters will be investigated. Meanwhile, more studies on the wavy path pattern to integrate the proposed methodology into current process planning of digital models for various AM technologies are required. For example, the thin-walled geometry can be recognised automatically from arbitrary models after its build orientation has been determined.

Acknowledgement

This paper is sponsored by the National Natural Science Foundation of China (number 51375440) and also sponsored by K.C. Wong Magna Fund in Ningbo University.

Disclosure statement

No potential conflict of interest was reported by the authors.

Funding

This paper is sponsored by the National Natural Science Foundation of China (number 51375440) and also sponsored by K.C. Wong Magna Fund in Ningbo University.

References

Abele, E., H. A. Stoffregen, M. Kniepkamp, S. Lang, and M. Hampe. 2015. “Selective Laser Melting for Manufacturing of Thin-Walled Porous Elements.” *Journal of Materials Processing Technology* 215 (1): 114–122. doi:10.1016/j.jmatprotec.2014.07.017.

Alexander, P., and D. Dutta. 2000. “Layered Manufacturing of Surfaces with Open Contours Using Localized Wall Thickening.” *CAD Computer Aided Design* 32 (3): 175–189. doi:10.1016/S0010-4485(99)00079-2.

Wohlers, T. 2015. *3D Printing and Additive Manufacturing State of the Industry*: Wohlers Report; Wohlers Associates Inc.: Fort Collins, CO, USA.

Blum, H. 1967. “A Transformation for Extracting New Descriptors of Shape.” In Proceedings of Models for the Perception of Speech and Visual Form (MIT Press, 1967), 362–380. doi:10.1142/S0218654308001154

Boschetto, A., and L. Bottini. 2016. “Design for Manufacturing of Surfaces to Improve Accuracy in Fused Deposition Modeling.” *Robotics and Computer-Integrated Manufacturing* 37: 103–114. doi:10.1016/j.rcim.2015.07.005.

Cacciola, F. 2004. *A CGAL Implementation of the Straight Skeleton of A Simple 2D Polygon with Holes*. In *2nd CGAL User Workshop*, Polytechnic Univ., Brooklyn, New York, USA, June 2004.

Cerit, E., and I. Lazoglu. 2011. “A CAM-Based Path Generation Method for Rapid Prototyping Applications.” *The International Journal of Advanced Manufacturing Technology* 56 (1–4): 319–327. doi:10.1007/s00170-011-3176-y.

Chen, Z. C., and Q. Fu. 2011. “An Optimal Approach to Multiple Tool Selection and Their Numerical Control Path Generation for Aggressive Rough Machining of Pockets with Free-Form Boundaries.” *Computer-Aided Design* 43 (6): 651–663. doi:10.1016/j.cad.2011.01.020.

Chou, C., Y. Chen, and S. Chou. 2008. “A Fundamental Tool Path Planning Problem for Circles in Layered Manufacturing.” *Integrated Computer-Adied Engineering* 15: 37–52.

Ding, D., Z. Pan, D. Cuiuri, and H. Li. 2014. “A Tool-Path Generation Strategy for Wire and Arc Additive Manufacturing.” *The International Journal of Advanced Manufacturing Technology* 73 (1–4): 173–183. doi:10.1007/s00170-014-5808-5.

Ding, D., Z. Pan, D. Cuiuri, and H. Li. 2015. “A Practical Path Planning Methodology for Wire and Arc Additive Manufacturing of Thin-Walled Structures.” *Robotics and Computer-Integrated Manufacturing* 34: 8–19. doi:10.1016/j.rcim.2015.01.003.

El-Midany, T. T., A. Elkeran, and H. Tawfik. 2006. “Toolpath Pattern Comparison Contour-Parallel with Direction-Parallel.” In *Proceedings of the Geometric Modeling and Imaging— New Trends*, Vol. 2006, 77–82. doi:10.1109/GMAI.2006.45.

Han, W., M. A. Jafari, S. C. Danforth, and A. Safari. 2002. “Tool Path-Based Deposition Planning in Fused Deposition Processes.” *Journal of Manufacturing Science and Engineering* 124 (2): 462. doi:10.1115/1.1455026.

Held, M. 1991. “A Geometry-Based Investigation of the Tool Path Generation for Zigzag Pocket Machining.” *The Visual Computer* 7 (5–6): 296–308. doi:10.1007/BF01905694.

Huang, B., and S. Singamneni. 2013. “Adaptive Slicing and Speed- and Time-Dependent Consolidation Mechanisms in Fused Deposition Modeling.” *Proceedings of the Institution of Mechanical Engineers, Part B: Journal of Engineering Manufacture* 228 (1): 111–126. doi:10.1177/0954405413497474.

Huang, X., C. Ye, S. Wu, K. Guo, and J. Mo. 2009. “Sloping Wall Structure Support Generation for Fused Deposition Modeling.” *The International Journal of Advanced Manufacturing Technology* 42 (11–12): 1074–1081. doi:10.1007/s00170-008-1675-2.

Jin, G. Q., W. D. Li, L. Gao, and K. Popplewell. 2013. “A Hybrid and Adaptive Tool-Path Generation Approach of Rapid Prototyping and Manufacturing for Biomedical Models.” *Computers in Industry* 64 (3): 336–349. doi:10.1016/j.compind.2012.12.003.

Jin, Y., Y. He, G. Xue, and J. Fu. 2014a. “A Parallel-Based Path Generation Method for Fused Deposition Modeling.” *The International Journal of Advanced Manufacturing Technology* 77 (5–8): 927–937. doi:10.1007/s00170-014-6530-z.

Jin, Y.-A., Y. He, J.-Z. Fu, W.-F. Gan, and Z.-W. Lin. 2014b. “Optimization of Tool-Path Generation for Material Extrusion-Based Additive Manufacturing Technology.” *Additive Manufacturing* 1: 32–47. doi:10.1016/j.addma.2014.08.004.

Kai, C. C., G. G. K. Jacob, and T. Mei. 1997a. “Interface between CAD and Rapid Prototyping Systems. Part 1: A Study of Existing Interfaces.” *The International Journal of Advanced Manufacturing Technology* 13 (8): 571–576. doi:10.1007/bf01176300.

Kai, C. C., G. G. K. Jacob, and T. Mei. 1997b. "Interface between CAD and Rapid Prototyping Systems. Part 2: LMI - an Improved Interface." *The International Journal of Advanced Manufacturing Technology* 13 (8): 571–576. doi:10.1007/BF01176301.

Kao, J., and F. B. Prinz. 1998. "Optimal Motion Planning for Deposition in Layered Manufacturing." In *1998 ASME Design Engineering Technical Conferences*, 1–10, Atlanta, Georgia, USA.

Kim, H. C. 2010. "Optimum Tool Path Generation for 2.5D Direction-Parallel Milling with Incomplete Mesh Model." *Journal of Mechanical Science and Technology* 24 (5): 1019–1027. doi:10.1007/s12206-010-0306-7.

Lee, D. T. 1982. "Medial Axis Transformation Of." *Pattern Analysis & Machine Intelligence IEEE Transactions* 4 (4):363-369.

Lee, E. 2003. "Contour Offset Approach to Spiral Toolpath Generation with Constant Scallop Height." *CAD Computer Aided Design* 35 (6): 511–518. doi:10.1016/S0010-4485(01)00185-3.

Lin, Z., J. Fu, Y. He, and W. Gan. 2013. "A Robust 2D Point-Sequence Curve Offset Algorithm with Multiple Islands for Contour-Parallel Tool Path." *CAD Computer Aided Design* 45 (3): 657–670. doi:10.1016/j.cad.2012.09.002.

Liu, X. Z., J. H. Yong, G. Q. Zheng, and J. G. Sun. 2007. "An Offset Algorithm for Polyline Curves." *Computers in Industry* 58 (3): 240–254. doi:10.1016/j.compind.2006.06.002.

Park, S. C., and B. K. Choi. 2000. "Tool-Path Planning for Direction-Parallel Area Milling." *CAD Computer Aided Design* 32 (1): 17–25. doi:10.1016/S0010-4485(99)00080-9.

Peng, L., J. Shengqin, Z. Xiaoyan, H. Qianwu, and X. Weihao. 2007. "Direct Laser Fabrication of Thin-Walled Metal Parts under Open-Loop Control." *International Journal of Machine Tools and Manufacture* 47 (6): 996–1002. doi:10.1016/j.ijmachtools.2006.06.017.

Reiner, T., N. Carr, R. Měch, O. Šťava, C. Dachsbacher, and G. Miller. 2014. "Dual-Color Mixing for Fused Deposition Modeling Printers." *Computer Graphics Forum* 33 (2):479–486. doi: 10.1111/cgf.12319

Steuben, J. C., A. P. Iliopoulos, and J. G. Michopoulos. 2016. "Implicit Slicing for Functionally Tailored Additive Manufacturing." *Computer-Aided Design* 77: 107–119. doi:10.1016/j.cad.2016.04.003.

Tang, K., and A. Pang. 2003. "Optimal Connection of Loops in Laminated Object Manufacturing." *CAD Computer Aided Design* 35 (11): 1011–1022. doi:10.1016/S0010-4485(02)00162-8.

Turner, B. N., R. Strong, and S. A. Gold. 2014. "A Review of Melt Extrusion Additive Manufacturing Processes: I. Process Design and Modeling." *Rapid Prototyping Journal* 20 (3): 192–204. doi:10.1108/RPJ-01-2013-0012.

Valkenaers, H., F. Vogeler, E. Ferraris, A. Voet, and J.-P. Kruth. 2013. "A Novel Approach to Additive Manufacturing: Screw Extrusion 3d-Printing." 4M Conference, (c), 235–238. http://rpsonline.com.sg/proceedings/9789810772475/html/359.xml

Wah, P. K., K. G. Murty, A. J. A. Y. Joneja, and L. C. H. I. Chiu. 2002. "Tool Path Optimization in Layered Manufacturing Tool Path Optimization in Layered Manufacturing." *IIE Transactions* 34 (4): 335–347. doi:10.1080/07408170208928874.

Wang, W., H. Chao, J. Tong, Z. Yang, X. Tong, H. Li, X. Liu, and L. Liu. 2015. "Saliency-Preserving Slicing Optimization for Effective 3D Printing." *Computer Graphics Forum* 34 (6): 148–160. doi:10.1111/cgf.12527.

Weidong, Y. W. Y. 2009. "Optimal Path Planning in Rapid Prototyping Based on Genetic Algorithm." *2009 Chinese Control and Decision Conference* 5068–5072. doi:10.1109/CCDC.2009.5194966.

Yang, Y., H. T. Loh, J. Y. H. Fuh, and Y. G. Wang. 2002. "Equidistant Path Generation for Improving Scanning Efficiency in Layered Manufacturing." *Rapid Prototyping Journal* 8 (1): 30–37. doi:10.1108/13552540210413284.

You, C.-F., B.-T. Sheen, and T.-K. Lin. 2001. "Robust Spiral Tool-Path Generation for Arbitrary Pockets." *International Journal of Advanced Manufacturing Technology* 17 (3): 181–188. doi:10.1007/PL00003944.

Zhao, H., Y. Chen, C. Tu, and B. Chen. 2016. "Connected Fermat Spirals for Layered Fabrication." *ACM Transactions on Graphics* 35 (4): 100:1–100: 10. doi:10.1145/2897824.2925958.

Zhou, B., J. Zhao, L. Li, and R. Xia. 2016. "Double Spiral Tool-Path Generation and Linking Method for Complex Pocket Machining." *Machining Science and Technology* 20 (2): 262–289. doi:10.1080/10910344.2016.1168928.